



Theoretical insights and implications of bouncing cosmology in $f(\mathcal{R}, T^2)$ theory

M. Sharif^a , M. Zeeshan Gul^b, I. Hashim^c

Department of Mathematics and Statistics, The University of Lahore, 1-KM Defence Road, Lahore 54000, Pakistan

Received: 5 September 2024 / Accepted: 9 October 2024

© The Author(s) 2024

Abstract In this paper, we explore cosmological bouncing solutions to investigate the cosmic evolution in the framework of energy-momentum squared gravity. We consider flat Friedmann–Robertson–Walker spacetime with a perfect matter distribution. We assume two different functional forms of $f(\mathcal{R}, T^2)$ gravity model to examine the impact of this modified framework in the evolution of the universe. Furthermore, we consider a specific scale factor to investigate different cosmological parameters, analyzing the evolutionary behavior of the universe in this gravity. We also perform stability analysis using the perturbation technique. Our findings indicate that the null energy condition violates at the bounce point and equation of state parameter exhibits characteristics of a quintessence era or phantom regimes. These aspects highlight the complex interplay between energy conditions and stability in bouncing cosmological model. We conclude that the $f(\mathcal{R}, T^2)$ theory successfully provides viable alternatives to the standard cosmological scenarios, offering insights into the early universe and the nature of gravity.

1 Introduction

General relativity (GR), formulated by Albert Einstein transformed our comprehension of gravity by defining it as the curvature of spacetime, resulting from the presence of matter and energy. This theory successfully explains a wide range of gravitational phenomena from planetary orbits to the dynamics of galaxies and the expansion of the universe. However, the accelerated cosmic expansion poses a challenge to GR as it relies on the cosmological constant to account for dark energy (DE), leading to the cosmological constant problem. This problem motivated researchers to modify GR by adding

or replacing the scalar invariants and their generic function in the Einstein–Hilbert action. These are alternative models that provide deep insights and explanation for phenomena such as DE, accelerated cosmic expansion and other cosmological as well as astrophysical observations. This allows for a richer set of dynamical behavior which can mimic DE and modify large-scale structure formation. The $f(\mathcal{R})$ theory is regarded as one of the simplest modifications of GR, which is obtained by replacing the Ricci scalar (\mathcal{R}) with a generic function in the Einstein–Hilbert action [1]. A thorough discussion of this theory and its implications is provided in [2]. There are different forms of modified theories such as curvature, torsion and non-metricity-based theories [3–18].

The presence of singularities is considered a major problem in GR because of its prediction at the high energy level, where GR is no longer valid due to the expected quantum impacts. However, there is no specific formalism for quantum gravity. In this regard, a new generalization of GR is recently proposed which allows a correction term $T^{\mu\nu}T_{\mu\nu}$ in the functional action known as energy-momentum squared gravity (EMSG). This is also referred to as $f(\mathcal{R}, T^2)$ theory, where T^2 is denoted by $T^{\mu\nu}T_{\mu\nu}$ [19]. In this framework, the gravitational action depends on the Ricci scalar and the contraction of the energy-momentum tensor (EMT), allowing for a more nuanced interaction between geometry and matter. The inclusion of extra non-linear terms provide the explanations for mysterious cosmic phenomena such as galactic rotation curves and large-scale structures without the need for dark matter [20]. It is worthwhile to mention here that EMSG reduces to GR in vacuum with its effects become significant only in regions of high curvature regime.

This modification of GR is considered the most favorable and prosperous technique which resolves the spacetime singularity in the non-quantum description. Consequently, the corresponding field equations are different from GR only in the presence of matter sources. It contributes squared terms

^a e-mail: msharif.math@pu.edu.pk (corresponding author)

^b e-mail: mzeeshangul.math@gmail.com (corresponding author)

^c e-mail: imran.hashim@math.uol.edu.pk

in the field equations that are used to explore various fascinating cosmological consequences. This theory has maximum energy density and correspondingly a minimum scale factor at the early universe which indicates that there is a bounce at early times. Moreover, this theory possesses a true sequence of cosmological eras. Although the cosmological constant does not play a crucial role in the background of the standard cosmological model, however, the cosmological constant supports resolving singularity only after the matter-dominated era in EMSG. However, the profile of density supports the inflationary cosmological models that successfully provide convincing answers to major cosmological issues like horizon problem, flatness problem, etc. It is worthwhile to mention here that this theory overcomes the spacetime singularity but does not change the cosmological evolution.

Roshan and Shojai [21] examined that EMSG has a bounce in the early times and resolves the primordial singularity. Board and Barrow [22] used a specific model of this theory and discussed exact solution, singularities as well as cosmic evolution with the isotropic configuration of matter in this theory. This novel approach passes the solar system tests [23]. It has garnered increasing interest from researchers due to its theoretical implications, consistency with observational data and significance in cosmological contexts [24–26]. Bahamonde et al. [27] studied various models of this theory and found that these models manifest the current evolution and acceleration of the cosmos. Ranjit et al. [28] examined possible solutions for matter density and discussed their cosmological results in EMSG. The analysis of observational constraints in alternatives theories of gravity has been examined in [29–44]. Sharif and his collaborators studied the Noether symmetry approach [45, 46], dynamics of gravitational collapse [47–53] and static spherically symmetric structures [54–57] in $f(\mathcal{R}, T^2)$ theory.

The cosmic observations determine that the universe started from singularity, known as big bang theory. This theory explains various observable phenomena, including the cosmic microwave background and the large-scale structures of the cosmos. However, it faces challenges such as the horizon and flatness problems [58]. To address these issues, the inflation theory was developed [59], which provides a basic explanation of the cosmic expansion. This theory successfully addresses all issues except singularity problem. In this perspective, a viable cosmic model has been developed to resolve the initial singularity, named as bouncing cosmology. Bouncing cosmology offers an alternative to big bang by proposing that the cosmos experiences cycles of contraction and expansion, avoiding the singularity issue [60, 61]. This model suggests that rather than a single beginning, the universe has experienced multiple cycles of expansion and contraction, providing a new perspective on cosmic evolution. Regarding to the bouncing behavior, the Hubble parameter must be negative before the bouncing point and positive after

the bouncing point. Bounce solutions are significant in the field of cosmology because they offer a way to solve the initial singularity. Moreover, this cosmological model provides an intriguing solution to the horizon and flatness problems without the need for an inflationary phase.

Bozza and Burni [62] addressed the anisotropy problem in bouncing cosmology. Cai et al. [63] proposed a nonsingular bouncing cosmology using a scalar field. Their model successfully achieves the “matter bounce” scenario and overcomes the anisotropy issue, providing a more robust framework for understanding the early stages of cosmic evolution. Cai [64] proposed the matter-bounce inflation scenarios with their reconstructed models. These models are anticipated to provide valuable insights into the future trajectory of observational cosmology. Bouncing cosmology in modified theories has attracted significant interest because of their intriguing features. Bamba et al. [65] explored $f(\mathcal{R})$ gravity using various forms of the scale factor to identify viable bouncing solutions in modified context. Moreover, bouncing cosmology in the context of modified Gauss–Bonnet gravity has been examined in [66]. Amani [67] studied the bouncing solution in $f(\mathcal{R})$ theory by redshift parameter. Haro and Amoros [68] considered the Arnowitt–Deser–Misner formalism to build bouncing cosmological solutions in $f(\mathcal{T})$ theory, where \mathcal{T} is the torsion scalar. Tripathy et al. [69] studied bouncing solutions in extended theory of gravity.

Shabani and Ziaie [70] explored the bouncing solutions in $f(\mathcal{R}, T)$ theory using flat Friedmann–Robertson–Walker (FRW) spacetime. Caruana et al. [71] investigated cosmological bouncing scenarios in the flat FRW geometry in $f(\mathcal{T}, B)$ theory, where B is the boundary term. Furthermore, the non-singular bouncing universe via null energy condition has been studied in [72]. Zubair et al. [73] observed that matter-bounce models remain stable only when using linear forms of the $f(\mathcal{R}, T)$ function, while reconstructed power law model remain unstable. Ganiou et al. [74] reconstructed $f(G)$ gravity model (G is the Gauss–Bonnet invariant) that characterize critical phases of cosmic evolution. Singh et al. [75] investigated bouncing scenario in $f(\mathcal{R}, T)$ gravity by parameterizing the scale factor. Sharif and his collaborators studied bouncing solutions in $f(Q)$ theory (Q characterizes non-metricity) [76, 77]. Recently, Gul et al. [78] generalized their work in $f(Q, T)$ and described the cosmic expansion in the vicinity of the bouncing point.

This manuscript provides a framework to study the cosmic evolution in EMSG. The layout of this paper is given as follows. Section 2 derives the field equations of EMSG in the presence of FRW spacetime. A comprehensive examination of bouncing solutions for different scenarios are presented in Sect. 3. The stability analysis is given in Sect. 4. Our main findings are summarized in Sect. 5.

2 $f(\mathcal{R}, T^2)$ theory and FRW spacetime

The corresponding action is given by

$$\mathcal{S} = \int d^4x \left(\frac{1}{2\kappa^2} f(\mathcal{R}, T^2) + L_m \right) \sqrt{-g}, \quad (1)$$

where $\kappa^2 = 1$ is the coupling constant, g demonstrates determinant of the metric tensor and L_m refers to the matter-Lagrangian density. The field equations are obtained by varying the action with respect to the metric tensor as

$$f_{T^2} \Theta_{\mu\nu} + \mathcal{R}_{\mu\nu} f_{\mathcal{R}} - \frac{1}{2} g_{\mu\nu} f + (g_{\mu\nu} \square - \nabla_\mu \nabla_\nu) f_{\mathcal{R}} = T_{\mu\nu}, \quad (2)$$

where

$$\Theta_{\mu\nu} = -4 \frac{\partial^2 L_m}{\partial g^{\mu\nu} \partial g^{\varphi\beta}} T^{\varphi\beta} - 2L_m (T_{\mu\nu} - \frac{1}{2} g_{\mu\nu} T) - TT_{\mu\nu} + 2T_\mu^\varphi T_{\nu\varphi}. \quad (3)$$

Here, $f_{\mathcal{R}} = \frac{\partial f}{\partial \mathcal{R}}$, $f_{T^2} = \frac{\partial f}{\partial T^2}$, $\square = \nabla^\epsilon \nabla_\epsilon$ and ∇_ϵ is the covariant derivative. Rearranging Eq. (2), we obtain

$$G_{\mu\nu} = \frac{1}{f_{\mathcal{R}}} (T_{\mu\nu} + T_{\mu\nu}^c), \quad (4)$$

where $G_{\mu\nu}$ represents the Einstein tensor and

$$T_{\mu\nu}^c = \frac{1}{2} g_{\mu\nu} (f - \mathcal{R} f_{\mathcal{R}}) - \Theta_{\mu\nu} f_{T^2} - (g_{\mu\nu} \square - \nabla_\mu \nabla_\nu) f_{\mathcal{R}}. \quad (5)$$

We assume perfect matter configuration as

$$T_{\mu\nu} = (\rho + p) \mathbb{U}_\mu \mathbb{U}_\nu - p g_{\mu\nu}, \quad (6)$$

where \mathbb{U}_μ denotes the four-velocity, ρ signifies the energy density and p represents the pressure. We assume $L_m = p$ [79], which simplifies the mathematical formulation, making it easier to derive the field equations and analyze solutions, while capturing essential features of the matter fields in cosmological context. By adopting this assumption, we effectively investigate the interplay between matter and geometry, leading to deep understanding of the universe dynamics in EMSG. Using $L_m = p$ in Eq. (3), we obtain

$$\Theta_{\mu\nu} = -(\rho^2 + 3p^2 + 4p\rho) \mathbb{U}_\mu \mathbb{U}_\nu. \quad (7)$$

To explore the enigmatic nature of the universe, we assume a flat FRW universe as

$$ds^2 = dt^2 - a^2(t) (dx^2 + dy^2 + dz^2), \quad (8)$$

where $a(t)$ represents the scale factor. Using Eqs. (2)–(8), the corresponding field equations become

$$3H^2 = \frac{1}{f_{\mathcal{R}}} \left[\rho + \frac{1}{2} (f(\mathcal{R}, T^2) - \mathcal{R} f_{\mathcal{R}}) \right. \\ \left. + f_{2T^2} (\rho^2 + 3p^2 + 4p\rho) - 3H\dot{\mathcal{R}} f_{\mathcal{R}\mathcal{R}} \right], \quad (9)$$

$$3H^2 + 2\dot{H} = \frac{1}{f_{\mathcal{R}}} \left[-p - \frac{1}{2} (f(\mathcal{R}, T^2) - \mathcal{R} f_{\mathcal{R}}) + \ddot{\mathcal{R}} f_{\mathcal{R}\mathcal{R}} \right. \\ \left. + \dot{\mathcal{R}}^2 \times f_{\mathcal{R}\mathcal{R}\mathcal{R}} - 2H\dot{\mathcal{R}} f_{\mathcal{R}\mathcal{R}} \right]. \quad (10)$$

These modified equations are essential for establishing a theoretical framework to comprehend cosmic mysteries. The $f(\mathcal{R}, T^2)$ gravity provides non-conserved EMT, implying the presence of an extra force that acts as a nongeodesic motion of particles given by

$$\nabla^\mu T_{\mu\nu} = \nabla^\mu \Theta_{\mu\nu} f_{T^2} - \frac{1}{2} g_{\mu\nu} \nabla^\mu f(T^2). \quad (11)$$

The non-conservation equation for perfect fluid turns out to be

$$\dot{\rho} + \frac{3\dot{a}}{a} (\rho + p) = (3p^2 + \rho^2 + 4p\rho) \dot{f}_{T^2} \\ - \frac{3\dot{a}}{a} (3p^2 + \rho^2 + 4p\rho) f_{T^2} \\ - f_{T^2} \{ \dot{\rho} (3\rho + 4p) + \dot{p} (9p + 4\rho) \}. \quad (12)$$

The non-conserved EMT shows that in $f(\mathcal{R}, T^2)$ theory, there is an exchange of energy between matter and the gravitational field due to the additional term. In the context of bouncing cosmology, this exchange plays a critical role in facilitating the bounce, helping the universe to avoid singularities. As a result, particles moving in this modified gravitational field do not follow geodesic lines. Instead, they experience an additional force acting normal to their four-velocity, which alters their motion and reflects the complex interaction between matter and spacetime in this framework. This behavior is essential for understanding the early universe dynamics and the bounce phenomenon.

In the following section, we employ two distinct functional forms to proceed with the analysis.

Model-I

First, we consider the functional form of this theory with arbitrary constant (β) as [19]

$$f(\mathcal{R}, T^2) = \mathcal{R} + 2\beta T^2. \quad (13)$$

This model introduces a simple extension to GR which allows for richer dynamics in the interaction between matter and geometry, offering new pathways to address DE, cosmic acceleration and the early universe behavior. The term \mathcal{R} in our choice of the functional form is standard in gravitational theories as it directly recovers GR in the limit where modifications vanish ($\beta = 0$). By maintaining this linear term, we ensure that the theory reduces to GR in low-energy regimes or in the absence of significant T^2 effects, thus making it

consistent with classical tests of gravity in well-understood regimes such as the solar system. The introduction of the T^2 term is motivated by the need to incorporate matter-geometry couplings that could explain certain cosmological phenomena. The quadratic dependence ensures that the corrections to the Einstein–Hilbert action become significant in the high-energy regimes of the early universe. This model aims to provide more accurate predictions for phenomena such as DE, dark matter and the early stages of the cosmic evolution, which remain enigmatic in the current theoretical paradigm. Moreover, this functional form aligns with broader theoretical endeavors, such as the quest for a quantum theory of gravity and a deep understanding of spacetimes fundamental nature. It reconciles theoretical predictions with experimental observations while offering a more comprehensive understanding of the cosmic evolution, particularly during its transition phases. By adopting this model, physicists can explore the possibility of avoiding cosmological singularities and better understand the fundamental laws that govern the cosmos.

Using Eqs. (9), (10) and (13), the corresponding field equations become

$$3H^2 = \rho + \beta(\rho^2 + 3p^2) + 2\beta(\rho^2 + 3p^2 + 4\rho p), \quad (14)$$

$$3H^2 + 2\dot{H} = p - \beta(\rho^2 + 3p^2). \quad (15)$$

Simultaneously these equations, we obtain the explicit expressions of matter contents as

$$\rho = -\frac{3}{16\beta} - \frac{1}{2}\sqrt{\frac{\Gamma^1}{\Gamma^2 + (192\sqrt[3]{2}\beta^3)^{-1}\Gamma^3 + \Gamma^4}} - \frac{1}{2}\sqrt{\frac{\Gamma^5}{\Gamma^3 + \Gamma^4} - \frac{\Gamma^6\Gamma^1}{\Gamma^2} + \frac{\Gamma^3}{192\sqrt[3]{2}\beta^3\Gamma^4}}, \quad (16)$$

$$p = \frac{1}{288\beta H^2 + 144\beta\dot{H} + 9} \times \left[\frac{6H^2 + 3\dot{H} - 27}{256\beta^2\sqrt{\frac{\Gamma^1}{\Gamma^6}}} - \frac{9H^2}{\beta\sqrt{\frac{\Gamma^1}{\Gamma^6}}} - \frac{27\dot{H}}{8\beta\sqrt{\frac{\Gamma^1}{\Gamma^6}}} + \frac{9}{8}\sqrt{\frac{\Gamma^1}{\Gamma^6}} + 4\sqrt[3]{2}\beta\frac{\sqrt{\frac{\Gamma^1}{\Gamma^6}}}{\sqrt[3]{\Gamma^3}} - 528\sqrt[3]{2}\beta^2H^2\frac{\sqrt{\frac{\Gamma^1}{\Gamma^6}}}{\sqrt[3]{\Gamma^3}} - 46080\sqrt[3]{2}\beta^3H^4\frac{\sqrt{\frac{\Gamma^1}{\Gamma^6}}}{\sqrt[3]{\Gamma^3}} - 424\sqrt[3]{2}\beta^2\dot{H}\frac{\sqrt{\frac{\Gamma^1}{\Gamma^6}}}{\sqrt[3]{\Gamma^3}} \right]$$

$$- 47616\sqrt[3]{2}\beta^3H^2\dot{H}\frac{\sqrt{\frac{\Gamma^1}{\Gamma^6}}}{\sqrt[3]{\Gamma^3}} - 12416\sqrt[3]{2}\beta^3\dot{H}^2\frac{\sqrt{\frac{\Gamma^1}{\Gamma^6}}}{\sqrt[3]{\Gamma^3}}$$

$$- \frac{\sqrt[3]{\Gamma^3}}{8\sqrt[3]{2}\beta}\sqrt{\frac{\Gamma^1}{\Gamma^6}} + 8\beta^2\left(\frac{\Gamma^1}{\Gamma^6}\right)^{\frac{3}{2}} + \frac{11}{4}\Delta^1$$

$$+ 48H\beta^2\Delta^1 + 32\beta\dot{H}\Delta^1$$

$$\begin{aligned} & - \frac{424\sqrt[3]{2}\beta^2\dot{H}\Delta^2 + 528\sqrt[3]{2}\beta^2H^2\Delta^2}{\Gamma^3} \\ & + \frac{46080\sqrt[3]{2}\beta^3H^4\Delta^2 + \Delta^2}{\Gamma^3} \\ & + \frac{424\sqrt[3]{2}\beta^2\dot{H}\Delta^2 + 528\sqrt[3]{2}\beta^2H^2\Delta^2}{\Gamma^3} \\ & + \frac{47616\sqrt[3]{2}\beta^3H^2\dot{H}\Delta^2 + \Delta^2}{\Gamma^3} \\ & + \frac{12416\sqrt[3]{2}\beta^3\dot{H}^2\Delta^2 + \Delta^2}{\Gamma^3} \\ & + \frac{\Gamma^3}{8\sqrt[3]{2}\beta}\Delta^2 + 6\beta\Delta^2 + 8\beta^2\left((\Delta^2)^2 - \frac{\Gamma^7}{\Delta^2}\right)^{\frac{3}{2}} \end{aligned} \quad (17)$$

where

$$\begin{aligned} \Delta^1 &= \sqrt{\frac{\Gamma^5}{\Gamma^2 + \Gamma^4 - 192\sqrt[3]{2}\beta^3\sqrt{\Gamma^1}} - \frac{\Gamma^7}{4\sqrt{\frac{\Gamma^1}{\Gamma^1 + (192\sqrt[3]{2}\beta^3\Gamma^4)^{-1}\Gamma^3}}}}, \\ \Delta^2 &= \sqrt{\frac{\Gamma^5}{\Gamma^6 - (192\sqrt[3]{2}\beta^3)^{-1}\Gamma^3} - \frac{\Gamma^7}{4\sqrt{\frac{\Gamma^1}{\Gamma^6}}}}. \end{aligned}$$

Model-II

We assume another functional form of this theory as [80]

$$f(\mathcal{R}, T^2) = \mathcal{R} + \alpha\mathcal{R}^2 + 2\beta T^2, \quad (18)$$

where α is a non-zero constant. The inclusion of the \mathcal{R}^2 term is inspired by higher-order curvature corrections which provides a mechanism to avoid the singularity by allowing a smooth transition between contraction and expansion phases. This model offers a rich framework for exploring deviations from GR, making it a strong candidate for modeling the early universe cosmology. Inserting this functional form into Eqs. (9) and (10), we obtain

$$3H^2 = \frac{1}{1 + 2\alpha\mathcal{R}} \left[\rho + \frac{1}{2}(-\alpha\mathcal{R}^2 + 2\beta T^2) + 2\beta(\rho^2 + 3p^2 + 4\rho p) - 6\alpha H\dot{R} \right], \quad (19)$$

$$3H^2 + 2\dot{H} = \frac{1}{1 + 2\alpha\mathcal{R}} \left[p - \frac{1}{2}(-\alpha\mathcal{R}^2 + 2\beta T^2) + 2\alpha\ddot{R} - 4\alpha H\dot{R} \right]. \quad (20)$$

Solving these equations, we get

$$\begin{aligned} \rho &= \frac{19}{104\beta} - \frac{1}{2}\sqrt{\frac{\Gamma^8 + \Gamma^9}{78(2\frac{2}{3}\beta^3)\Gamma^{10}}} + \frac{\Gamma^{10}}{2496\sqrt[3]{2}\beta^3} \\ & - \frac{1}{2}\left[\Gamma^{11} - \frac{\Gamma^9}{78(2\frac{2}{3}\beta^3)\Gamma^{10}} - \frac{\Gamma^{10}}{2496(2\frac{2}{3}\beta^3)}\right] \end{aligned}$$

$$-\frac{\Gamma^{12}}{4\sqrt{\Gamma^{13} + \frac{\Gamma^9}{78(2^{\frac{2}{3}}\beta^3)\Gamma^{10}}}} + \frac{\Gamma^{10}}{2496\sqrt[3]{2}\beta^3} \Bigg]^{\frac{1}{2}}, \quad (21)$$

$$p = \left[-10\alpha\mathcal{R}^2 - 40\alpha\ddot{\mathcal{R}} - 60\alpha H^2\mathcal{R} - 30H^2 - 100\alpha H\dot{\mathcal{R}} \right. \\ + 80\alpha\dot{H}\mathcal{R} + 40\dot{H} - 15\alpha\mathcal{R}^2 + 30 \\ \times \left(\Delta^3 - \frac{\Gamma^{14}}{4\sqrt{\Gamma^{11} + \Gamma^{10}}} + \frac{\Gamma^{10}}{2496\sqrt[3]{2}\beta^3} \right) - 1098 \\ \times H^2\beta\Delta^3 - \frac{\Delta^3}{2496\sqrt[3]{2}\beta^3} - \frac{1}{2}\Delta^4 - 4392\alpha\beta H^2\mathcal{R}\Delta^4 \\ + \sqrt{\frac{\Gamma^{12} - \Gamma^{10}}{2496\sqrt[3]{2}\beta^3}} - \frac{3}{2}\sqrt{\frac{\Gamma^{11} - \Gamma^9}{78(2^{\frac{2}{3}}\beta^3)\Gamma^{10}}} \\ - \frac{1}{2496\sqrt[3]{2}\beta^3}\sqrt{\frac{\Gamma^{11} - \Gamma^9}{78(2^{\frac{2}{3}}\beta^3)\Gamma^{10}}} \\ - \frac{\Gamma^{12}}{\sqrt{\frac{\Gamma^{11} - \Gamma^9}{78(2^{\frac{2}{3}}\beta^3)\Gamma^{10}}}} + \frac{\Gamma^{12} - \Gamma^{10}}{416\sqrt[3]{2}\beta^3} - 18\alpha\beta\mathcal{R}^2\Delta^3 \\ - \frac{1}{2}\sqrt{\frac{\Gamma^9 + \Gamma^{11}}{78(2^{\frac{2}{3}}\beta^3)\Gamma^{10}}} + 174\alpha\mathcal{R}^2\beta\Delta^3 - 696\beta\dot{H}\Delta^5 \\ - 1392\alpha\beta\mathcal{R}\dot{H}\Delta^5 - 1500\alpha\beta H\dot{\mathcal{R}}\Delta^5 + 696\alpha\ddot{\mathcal{R}}\beta\Delta^5 \\ + 98\beta\Delta^5 - 312\beta^2\Delta^5 \Big] \\ \times \left[-180\alpha\mathcal{R}^2\beta - 720\alpha\ddot{\mathcal{R}}\beta + 1404\beta H^2 \right. \\ + 2808\alpha\beta H^2\mathcal{R} + 720\beta\dot{H} + 2088 \\ \times \alpha\beta H\dot{\mathcal{R}} + 1440\alpha\beta\dot{H}\mathcal{R} + 54\alpha\beta\mathcal{R}^2 - 20 \Big]^{-1}, \quad (22)$$

where

$$\Delta^3 = \frac{19}{104\beta} - \frac{1}{2} \left[\Gamma^{13} + \frac{\Gamma^9}{78(2^{\frac{2}{3}}\beta^3)\Gamma^{10}} + 359424\beta^3 \right. \\ \times \left(-70\alpha\mathcal{R}^2\beta - 280\alpha\ddot{\mathcal{R}}\beta \right. \\ \left. + 402\beta H^2 + 804\alpha\beta H^2\mathcal{R} + 280\beta\dot{H} + 524\alpha\beta H\dot{\mathcal{R}} \right. \\ \left. + 560\alpha\beta\dot{H}\mathcal{R} - 3\alpha \times \beta\mathcal{R}^2 - 10 \right)^2 - \Gamma^{10} \Bigg]^{\frac{1}{2}},$$

$$\Delta^4 = \left[\left(\frac{\Gamma^{11}}{78(2^{\frac{2}{3}}\beta)\Gamma^{10}} - \frac{\Delta^3}{2496\sqrt[3]{2}\beta^3} - \frac{\Gamma^{14}}{4\sqrt{\frac{\Gamma^9 + \Gamma^{13}}{(782^{\frac{2}{3}}\beta^3)\Gamma^{10}}}} \right)^{\frac{1}{2}} \right],$$

$$\Delta^5 = \left[\frac{19}{104\beta} - \frac{1}{2}\sqrt{\frac{\Gamma^8 + \Gamma^9}{78(2^{\frac{2}{3}}\beta^3)\Gamma^{10}}} + \frac{\Gamma^{11} - \Gamma^{10}}{2496\sqrt[3]{2}\beta^3} \right. \\ \left. - \frac{1}{2}\left[\sqrt{\frac{\Gamma^8 + \Gamma^9}{78(2^{\frac{2}{3}}\beta^3)\Gamma^{10}}} + \frac{\Gamma^{11} - \Gamma^{10}}{2496\sqrt[3]{2}\beta^3} \right] \right].$$

The values of $\Gamma^1 - \Gamma^{14}$ are given in Appendix A.

3 Comprehensive study of bouncing solutions

Bouncing solutions present a fascinating approach to resolve cosmological singularities such as the big bang, allowing the universe to undergo a non-singular bounce. This approach provides a framework where the universe transitions smoothly from a contracting phase to an expanding one, avoiding the initial singularities. This elegant mechanism not only offers an alternative to the standard cosmological model but also opens up new possibilities for understanding the early universe and the nature of cosmic evolution. The given constraints must be satisfied for a realistic bouncing pattern of the universe.

- The decreasing nature of the scale factor indicates that the universe is in a phase of contraction, while its increasing behavior signifies the era of cosmic expansion. If the bouncing model is non-singular then the scale factor should be minimum close to the bouncing point.
- The universe experiences contraction when Hubble parameter is negative and cosmos undergoes expansion when Hubble parameter is positive. The Hubble parameter vanishes at the bouncing point.
- The energy density must be positive, finite as well as maximum and pressure should be negative for the existence of non-singular bounce.

In the given subsections, a specific functional form of the scale factor is considered to achieve a successful bounce. This approach aims to solve the gravitational field equations under the assumption of no initial singularity in the universe.

3.1 Scale factor

The evolution of scale factor is crucial as it helps to understand how cosmos expands, contracts, or experiences a bouncing phase. This function plays a key role to examine the dynamics of cosmos with time. To develop a bouncing cosmological model, we adopt the scale factor as [81]

$$a(t) = (\gamma + \delta t^2)^{1/n}, \quad (23)$$

where γ , δ and n are non-zero constants. Using the values ($\delta = 2.5, 3.5, 4$), ($n = 0.5, 1.5, 2.5$) and ($\gamma = 1.2, 1.4, 1.8$), Fig. 1 determines the evolution of scale factor with time. The plot in this figure manifests that the behavior of scale factor is positive and symmetric which indicates the balance decreases and increases on both sides of the bouncing point. Additionally, the scale factor approaches to a non-zero minimum value near the bouncing point.

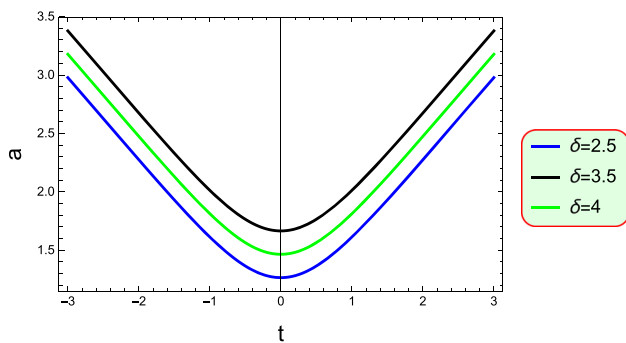


Fig. 1 Evolution of scale factor against t

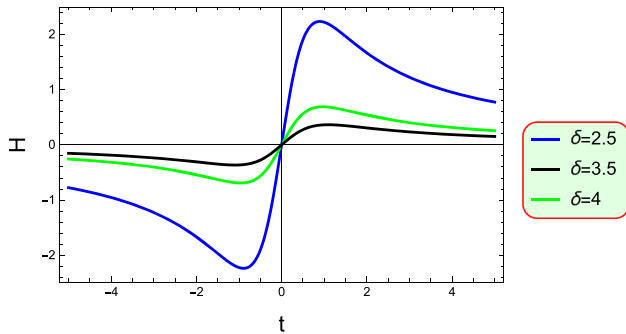


Fig. 2 Plot of Hubble parameter versus t for different parametric values

3.2 Hubble parameter

The Hubble parameter plays a vital role in the study of cosmic evolution, serving as a key observational quantity that describes the rate of cosmic expansion. Using Eq. (23), the Hubble parameter becomes

$$H = \frac{\dot{a}}{a} = \frac{2\delta t}{n(\gamma + \delta t^2)}. \quad (24)$$

Fig. 2 presents a graphical analysis of the Hubble parameter with time. The Hubble parameter is negative in the pre-bounce phase ($t < 0$), indicating a contracting universe and Hubble parameter vanishes at the bounce point. In the post-bounce phase ($t > 0$), the Hubble parameter becomes positive, indicating that the universe is now expanding. The transition of H from negative to positive values, passing through zero at the bounce, exemplifies the non-singular nature of the bouncing cosmology model. The graphical behavior of time derivative of the Hubble parameter shows transition in contraction and expansion phases of the cosmos as shown in Fig. 3.

3.3 Deceleration parameter

The deceleration parameter (q) is a significant cosmographic quantity that determines the rate of cosmic expansion. For $q > 0$, the universe experiences decelerated expansion, while

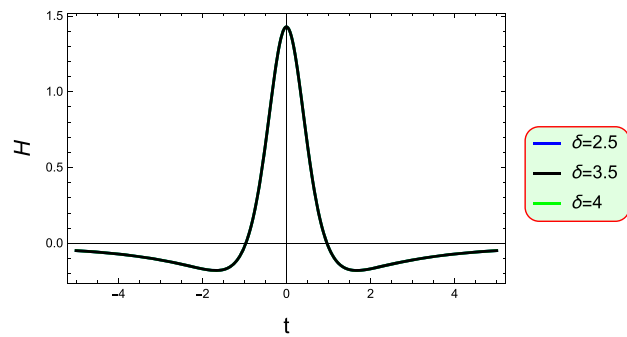


Fig. 3 Evolution of \dot{H} against t

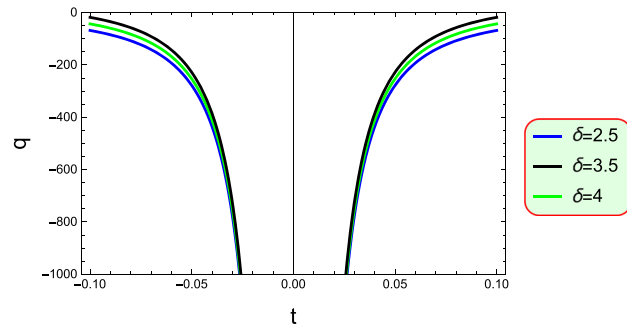


Fig. 4 Plot of deceleration parameter for different parametric values

$q < 0$ indicates accelerated cosmic expansion. Using Eq. (24), the deceleration parameter turns out to be

$$q = -1 - \dot{H}H^{-2} = \frac{1}{2} \left(-\frac{\gamma n}{\delta t^2} + n + 2 \right). \quad (25)$$

Figure 4 provides the graphical analysis of the deceleration parameter, highlighting a behavior consistent with the cyclic nature. Before and after the bounce phase, the deceleration parameter is negative, indicating that the universe expansion is accelerating. This behavior suggests that the forces driving the universe expansion post-bounce are similar to those acting during the pre-bounce contraction, leading to a consistent negative value of this parameter before and after the bounce. This negative value reflects the influence of factors driving the universe towards the bounce. At the bounce point, the deceleration parameter diverges, which shows a major change in the cosmic behavior, marking the exact moment of the bounce. This determines the dynamic and cyclical nature of the universe in bouncing cosmology.

3.4 Energy density and pressure

The energy density for both the models is computed by substituting Eqs. (23) and (24) into Eqs. (16) and (21), respectively. The resulting energy densities in the background of EMSG are plotted in Fig. 5. The pressure for both models is determined by inserting Eqs. (23) and (24) into Eqs. (17) and (22), respectively and depicted in Fig. 6. In bouncing cosmology,

the graphical analysis of energy density and pressure provide valuable insights into the nature of bounce, the behavior of the cosmos near the bounce point and the viability of different bouncing scenarios proposed in theoretical models. These graphical representations help us to understand the dynamics of the early universe. Prior to the bouncing epoch, the behavior of the energy density depends on the specific cosmological model being studied. For this case, the graphical behavior of the energy density and pressure is discussed for both models. Figures 5 and 6 show that the energy density consistently displays positive behavior for both considered models while pressure shows negative behavior which also aligns with the characteristics expected from the DE model.

3.5 Equation of state parameter

The equation of state (EoS) parameter ($\omega = \frac{p}{\rho}$) serves as a crucial parameter in understanding the fundamental nature of cosmic evolution. It provides a direct link between the pressure and density of the universe constituents, revealing how different cosmic components interact and influence the overall dynamics. By examining the EoS parameter, we can gain insights into the driving forces behind cosmic acceleration or deceleration, unraveling the mysteries of the cosmic expansion. This parameter helps us to understand the underlying physics of different cosmological models and also reveals the future trajectory of our universe. Its analysis is essential for bridging theoretical predictions with observational data, offering a clearer picture of the cosmos and its evolving nature. This parameter corresponds to different cosmic eras, i.e., $\omega = 0, 1/3, 1$ represent dust, radiation and stiff matter dominated era, respectively. It also determines the different expanding phases of the cosmos such as $-1 < \omega < -1/3$ represents quintessence and $\omega < -1$ portrays phantom regime.

Figure 7 shows that the EoS for model-II exhibits a significantly negative value, though it is less than -1 . This high negative value suggests that model-II is operating in a regime where the pressure is strongly negative compared to the energy density, indicating an exotic matter scenario or a strongly accelerating universe. Physically, this could imply that model-II is associated with a phase where the cosmic expansion is dominated by a form of energy or matter that has unusual properties, leading to accelerated expansion or even scenarios like a cosmological constant or DE. This behavior could also suggest that the model aligns with alternative cosmological models where the dynamics of the universe deviate from standard expectations. For model-I, the EoS parameter is greater than -1 . Thus, the graphical analysis reveals that both models exhibit accelerated expansion before and after the bounce, but model-I aligns with quintessence cosmology, while model-II corresponds to the phantom regime.

3.6 Analysis of null energy condition

The energy conditions serve as viable constraints with specific physical properties based on the EMT, which are employed to assess the physical consistency of cosmic models. Researchers have evaluated the viability of various cosmic configurations by imposing these constraints. These energy bounds are classified as null ($0 \leq \rho + p$), dominant ($0 \leq \rho - p$), weak ($0 \leq \rho, 0 \leq \rho + p$) and strong energy conditions ($0 \leq \rho + p, 0 \leq \rho + 3p$). Here, we explore the graphical behavior of the null energy constraint for the considered EMSG models. Violation of the null energy condition yields the violation of all energy conditions. Figures 8 depicts that the null energy constraint is negative before and after the bounce point. This violation is interpreted as an indication of a non-singular bounce that allows the universe to transition from a contracting phase to an expanding phase without encountering a singularity.

4 Stability analysis

The stability of the bouncing cosmological is investigated through linear homogeneous perturbations, which is crucial to understand the model's resilience to small fluctuations in the cosmological background. By examining the model response to these perturbations, we can evaluate its effectiveness as a theoretical framework for describing the cosmic dynamics. Additionally, assessing stability helps us to determine the conditions under which the model solutions remain consistent and reliable, offering valuable insights to explain accelerated cosmic expansion. For this purpose, we consider a general solution expressed as $H(t) = H^h(t)$ [82]. We analyze the model using this arbitrary solution, where the energy density and Hubble parameter can be perturbed as

$$H(t) = H^h(t)(1 + \eta(t)), \quad \rho(t) = \rho^h(1 + \eta^m(t)). \quad (26)$$

The first perturbation equation for the conserved EMT is [14]

$$\dot{\eta}^m(t) + 3H^h(t)\eta(t) = 0. \quad (27)$$

The second perturbation equation is obtained by inserting Eq. (26) into (17) and (23) and plotted in the Fig. 9 for model-I. This determines the behavior of the perturbation parameters η^m and η as a function of z in the context of the bouncing cosmological model. The graphs show that both perturbation parameters decrease and approach to zero as $z \rightarrow -1$, indicating minimal perturbations in the early stages of the cosmic evolution. As the universe undergoes a bounce, these parameters remain positive, signifying the robustness of the model against small perturbations. In the late time, the perturbation parameters continue to exhibit stable behavior, reinforcing the stability of the bouncing cosmological model under linear perturbations. Substituting Eq. (26) into (21) and solving

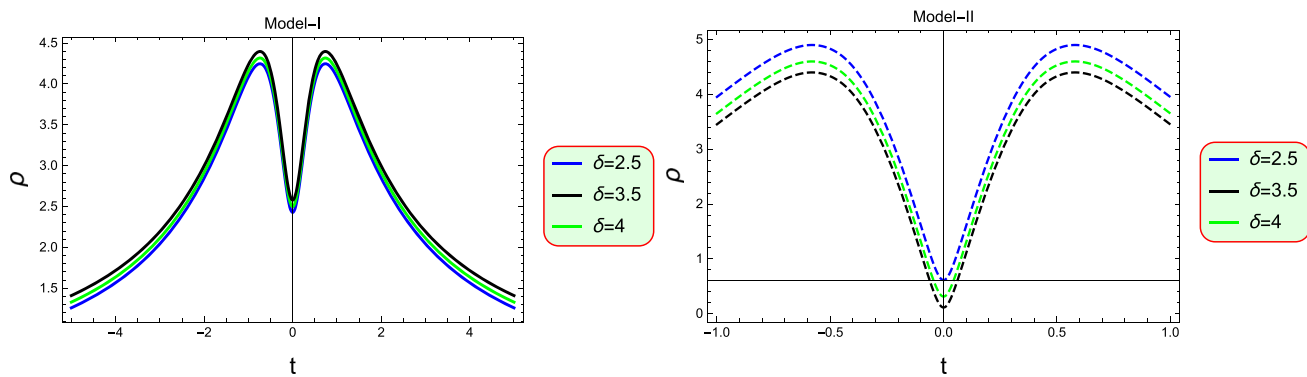


Fig. 5 The graphical behavior of energy density parameter versus t for different parametric values

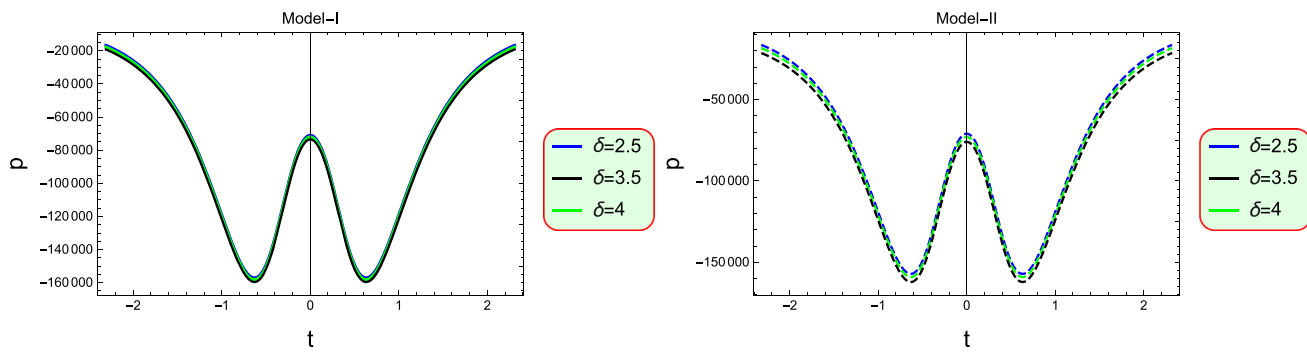


Fig. 6 The graphical behavior of pressure versus t for different parametric values

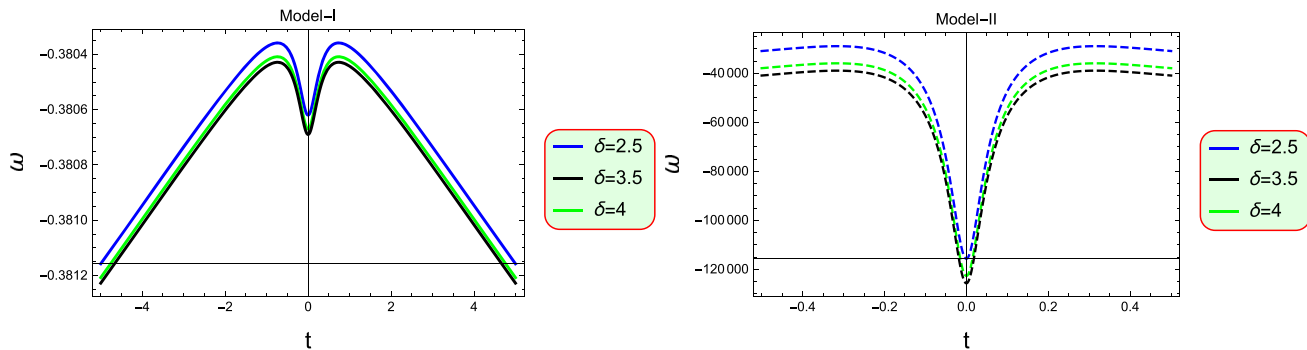


Fig. 7 Evolution of ω for different parametric values

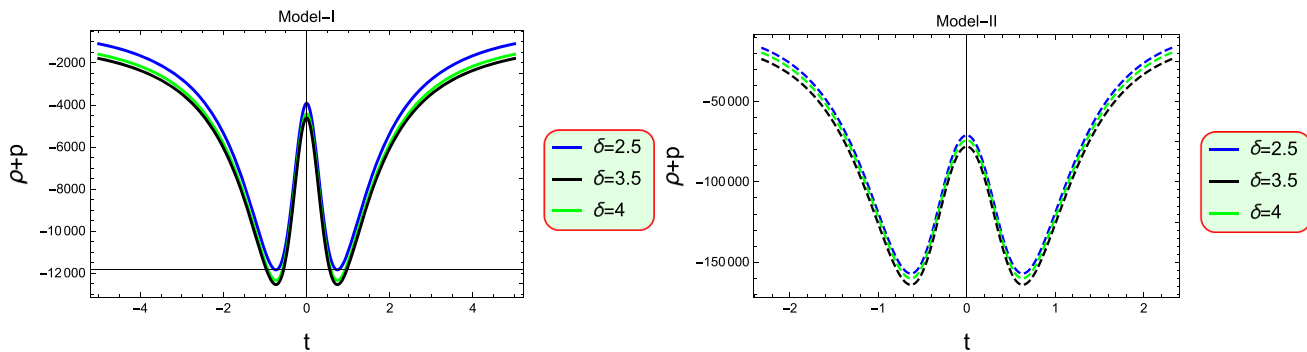


Fig. 8 Graphical behavior of null energy condition verses time

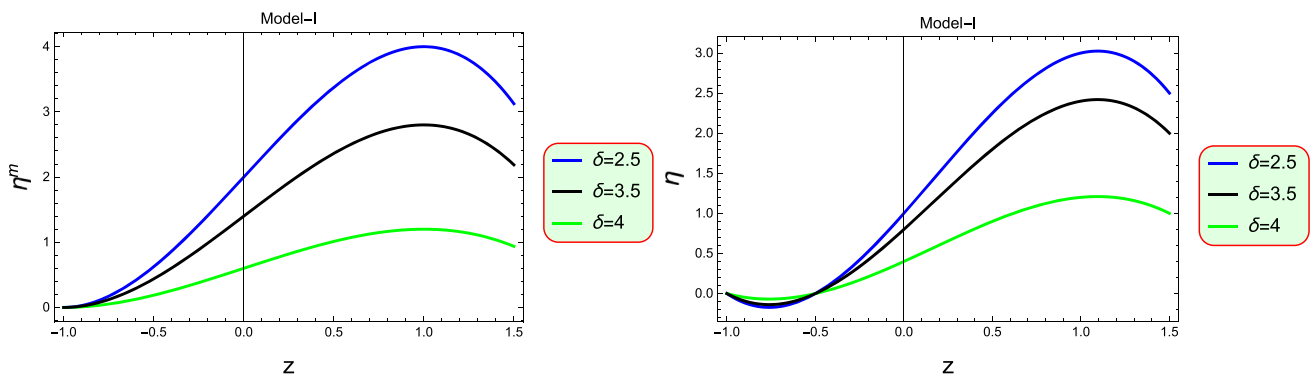


Fig. 9 Evolution of $\eta^m(z)$ and $\eta(z)$ against redshift variable for model-I

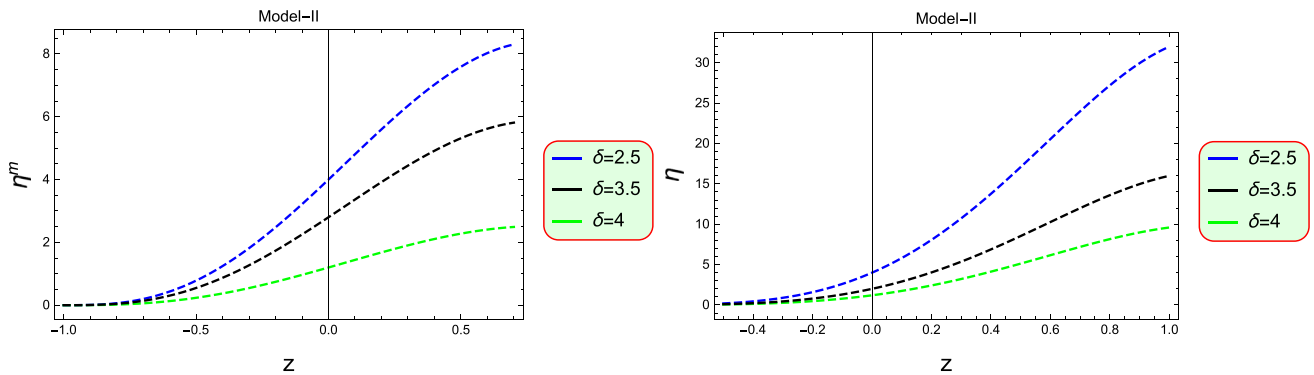


Fig. 10 Graphical evolution of η^m and η against redshift

it with (27), the perturbation parameters η and η^m are determined and depicted in Fig. 10 for model-II. The graphs in Fig. 10 demonstrate that the perturbation parameters follow a pattern similar to that observed in model-I.

5 Conclusions

In the recent years, the questions about the cosmic origin and evolution have been subject of great interest for cosmologist due to the limited observational data and mysterious aspects. In this regard, cosmologists have turned to bouncing cosmology as an appealing approach to address the challenges posed by the inflationary paradigm in the light of uncertainties regarding initial conditions and singularities at the outset of the big bang model. Our investigation has been focused on exploring viable bouncing models in a newly proposed EMSG framework. This study focuses on examining the well-known bouncing cosmological models in a FRW spacetime using a perfect matter distribution.

The extension to $f(\mathcal{R}, T^2)$ gravity is motivated by the need to explore modifications of GR that incorporate both quantum corrections and cosmological phenomena such as bouncing scenarios, which aim to address the singularity problem inherent in GR. This theory offers a modified gravi-

tational action where the non-minimal coupling between the Ricci scalar and self-contraction of the EMT introduces additional degrees of freedom. These degrees of freedom can be interpreted as contributing to the effective energy density and pressure, which can lead to the required violation of energy conditions and consequently facilitate a nonsingular bouncing solution. The choice of $f(\mathcal{R}, T^2)$ is based on the idea that interactions between matter and geometry could play a key role in the early universe. While $f(\mathcal{R})$ theory modifies the geometric side of the Einstein field equations, the inclusion of T^2 reflects a further coupling with the matter content. In many early-universe models, high-energy conditions can induce non-linear matter terms, and the T^2 term provides a phenomenological approach to capture such interactions.

Specifically, it allows for a more detailed modeling of energy-matter couplings, which are essential in high-energy cosmological regimes, like the ones expected in bouncing cosmology. The introduction of higher-order terms like T^2 can be viewed as an attempt to incorporate quantum corrections to the classical theory of gravity. In several quantum gravity approaches, corrections to the Einstein–Hilbert action are expected to emerge, which could include terms depending on the EMT. By introducing $f(\mathcal{R}, T^2)$, we aim to explore a class of modifications that could encapsulate such quantum effects in a phenomenological way, potentially leading to

new insights into the early universe dynamics. This extension aims to address cosmological challenges while maintaining consistency with observational data, especially in the context of early universe phenomena. Thus, the physical motivation behind using $f(\mathcal{R}, T^2)$ gravity lies in the desire to explore non-singular cosmological models, account for higher-order matter couplings and incorporate quantum corrections into the classical gravitational framework. This approach not only addresses the initial singularity problem but also provides a more comprehensive model for the interaction between matter and geometry in the early universe.

The scale factor reaches its minimum size, becomes non-zero and starts increasing, which explains the bouncing behavior during the early stages of cosmic evolution (Fig. 1). The Hubble parameter becomes negative during the pre-bounce phase, which indicates a contracting cosmos. As the universe approaches to the bouncing point ($t = 0$), the Hubble parameter vanishes. Moving into the post-bounce epoch, the Hubble parameter becomes positive, signifying the cosmic expansion (Fig. 2). We have seen the dynamic nature of the considered cosmic model as it transits between contraction and expansion phases (Fig. 3). There is a positive energy density and negative pressure, aligning with the anticipated accelerated expanding behavior of the cosmos as postulated by the DE model (Figs. 4, 5, 6). The EoS parameter falls in the quintessence and phantom regions near the bounce point (Fig. 7). Furthermore, we have discussed the cosmic acceleration and expansion through null energy condition in this framework. The null energy condition is violated for both models which confirms the existence of viable bouncing model in this theoretical framework (Fig. 8). Finally, we have studied the stability of both the models. The stability of the perturbation parameters over time confirms the robustness of the model against small perturbations, reinforcing its consistency and viability as a theoretical framework for describing cosmic evolution (Figs. 9, 10).

This research is focused on the idea of a bouncing cosmology in $f(\mathcal{R}, T^2)$ gravity which provides important perspectives for future investigations into the early development of the universe. These modified field equations using a variety of scale factors can offer a more effective way to analyze the present cosmological scenario. We have looked at how the results from the standard cosmological models match or differ. This aspect provides a more comprehensive knowledge of cosmological ideas and observational evidence. Gul et al. [78] studied the cosmological bouncing solutions in $f(Q, T)$ theory but they did not check stability. We have also checked stability of the system. It is found that our results are more consistent with observational data.

Funding There is no funding information for this research.

Data Availability Statement No data was used for the research described in this paper.

Code Availability Statement My manuscript has no associated code /software. [Authors' comment: Code/Software sharing not applicable to this article as no code/software was generated or analysed during the current study.]

Open Access This article is licensed under a Creative Commons Attribution 4.0 International License, which permits use, sharing, adaptation, distribution and reproduction in any medium or format, as long as you give appropriate credit to the original author(s) and the source, provide a link to the Creative Commons licence, and indicate if changes were made. The images or other third party material in this article are included in the article's Creative Commons licence, unless indicated otherwise in a credit line to the material. If material is not included in the article's Creative Commons licence and your intended use is not permitted by statutory regulation or exceeds the permitted use, you will need to obtain permission directly from the copyright holder. To view a copy of this licence, visit <http://creativecommons.org/licenses/by/4.0/>.

Funded by SCOAP³.

Appendix A

The values of Γ factors are given by

$$\begin{aligned}\Gamma^1 = & \frac{9}{64\beta^2} - \frac{48\beta H^2 + 32\beta \dot{H} + 5}{16\beta^2} \\ & + \frac{5\beta + 48\beta^2 H^2 + 32\beta^2 \dot{H}}{48\beta^3} + (-\beta^2 + 11520\beta^4 H^4 \\ & + 11904\beta^4 H^2 \dot{H} + 132\beta^3 H^2 + 3104\beta^4 \dot{H}^2 \\ & + 106\beta^3 \dot{H}), \\ \Gamma^2 = & \left[3 \times 2^{\frac{2}{3}} \beta^3 \left(15552\beta^3 (8\beta H^2 - 4\beta \dot{H} - 1)^2 \right. \right. \\ & \left. \left. + 5184\beta^2 (5\beta + 48\beta^2 H^2 + 32\beta^2 \dot{H}) \right. \right. \\ & \times (8\beta H^2 - 4\beta \dot{H} - 1) + 128(5\beta + 48\beta^2 H^2 \\ & + 32\beta^2 \dot{H})^3 + 559872\beta^4 (48\beta H^4 \\ & + 48\beta \dot{H} H^2 - H^2 + 12\beta \dot{H}^2) \\ & - 165888\beta^3 (5\beta + 48\beta^2 H^2 + 32\beta^2 \dot{H}) (48\beta H^4 \\ & + 48\beta \dot{H} H^2 - H^2 + 12\beta \dot{H}^2) \\ & + \left(4 - (-32\beta^2 + 368640\beta^4 H^4 + 380928\beta^4 H^2 \dot{H} \right. \\ & \left. + 4224\beta^3 H^2 + 99328\beta^4 \dot{H}^2 + 3392\beta^3 \dot{H})^3 \right. \\ & \left. + \left(15552\beta^3 (8\beta H^2 - 4\beta \dot{H} - 1)^2 + 5184\beta^2 \right. \right. \\ & \times (8\beta H^2 - 4\beta \dot{H} - 1) (5\beta + 48\beta^2 H^2 + 32\beta^2 \dot{H}) \\ & + 128(5\beta + 48\beta^2 H^2 + 32\beta^2 \dot{H})^3 \\ & + 559872\beta^4 (48\beta H^4 + 48\beta \dot{H} H^2 - H^2 + 12\beta \dot{H}^2) \\ & - 165888\beta^3 (5\beta + 48\beta^2 H^2 + 32\beta^2 \dot{H}) \\ & \left. \times (-H^2 + 48\beta H^4 + 48\beta \dot{H} H^2 - H^2 \right)\end{aligned}$$

$$\begin{aligned}
& +12\beta\dot{H}^2\Big)\Big)^2\Big)^{\frac{1}{2}}\Big)^{\frac{1}{3}}\Big], \\
\Gamma^3 = & \Big[(15552\beta^3(8\beta H^2 - 4\beta\dot{H} - 1)^2 \\
& + 5184\beta^2(8\beta H^2 - 4\beta\dot{H} - 1) \\
& (5\beta + 48\beta^2 H^2 + 32\beta^2 \\
& \times \dot{H}) + 128(5\beta + 48\beta^2 H^2 + 32\beta^2 \dot{H})^3 + 559872\beta^4 \\
& (48\beta H^4 + 48\beta\dot{H}H^2 - H^2 + 12\beta \\
& \times \dot{H}^2) - 165888\beta^3(5\beta + 48\beta^2 H^2 + 32\beta^2 \dot{H}) \\
& (48\beta H^4 + 48\beta\dot{H}H^2 - H^2 + 12\beta\dot{H}^2) + \Gamma^2\Big)^2, \\
\Gamma^4 = & \Big[4 - (-32\beta^2 + 368640\beta^4 H^4 \\
& + 380928\beta^4 H^2 \dot{H} + 4224\beta^3 H^2 + 99328\beta^4 \dot{H}^2 \\
& + 3392\beta^3 \dot{H})^3 + (15552\beta^3(8\beta H^2 - 4\beta\dot{H} - 1)^2 \\
& + 5184\beta^2(8\beta H^2 - 4\beta\dot{H} - 1) \\
& \times (5\beta + 48\beta^2 H^2 + 32\beta^2 \dot{H}) \\
& + 128(5\beta + 48\beta^2 H^2 + 32\beta^2 \dot{H})^3 \\
& + 559872\beta^4(48\beta H^4 \\
& + 48\beta\dot{H}H^2 - H^2 + 12\beta\dot{H}^2) - 165888\beta^3 \\
& (5\beta + 48\beta^2 H^2 + 32\beta^2 \dot{H})(-H^2 \\
& + 48\beta H^4 + 48\beta\dot{H}H^2 - H^2 + 12\beta\dot{H}^2)\Big)^2\Big)^{\frac{1}{2}}\Big)^{\frac{1}{3}}\Big], \\
\Gamma^5 = & \Big[\frac{9}{32\beta^2} - \frac{48\beta H^2 + 32\beta\dot{H} + 5}{16\beta^2} \\
& + \frac{5\beta + 48\beta^2 H^2 + 32\beta^2 \dot{H}}{48\beta^3} + (-\beta^2 + 11520\beta^4 H^4 \\
& + 11904\beta^4 H^2 \dot{H} \\
& + 132\beta^3 H^2 + 3104\beta^4 \dot{H}^2 + 106\beta^3 \dot{H})\Big], \\
\Gamma^6 = & \Big[\Gamma^1 + \frac{1}{192\sqrt[3]{2}\beta^3}\Big(15552\beta^3(8\beta H^2 - 4\beta\dot{H} - 1)^2 \\
& + 5184\beta^2(8\beta H^2 - 4\beta\dot{H} - 1)(5\beta \\
& + 48\beta^2 H^2 + 32\beta^2 \dot{H}) \\
& + 128(5\beta + 48\beta^2 H^2 + 32\beta^2 \dot{H})^3 \\
& + 559872\beta^4(48\beta H^4 + 48\beta\dot{H}H^2 \\
& - H^2 + 12\beta\dot{H}^2) - 165888\beta^3(5\beta \\
& + 48\beta^2 H^2 + 32\beta^2 \dot{H}) \\
& (48\beta H^4 + 48\beta\dot{H}H^2 - H^2 + 12\beta\dot{H}^2) + \Gamma^2\Big)^2, \\
& + 12\beta\dot{H}^2\Big)\Big)^2\Big)^{\frac{1}{2}}\Big)^{\frac{1}{3}}\Big],
\end{aligned}$$

$$\begin{aligned}
& \times \dot{H}^2) + \Gamma^2\Big)\Big], \\
\Gamma^7 = & -\frac{27}{64\beta^3} + \frac{3(48\beta H^2 + 32\beta\dot{H} + 5)}{16\beta^3} \\
& + \frac{3(8\beta H^2 - 4\beta\dot{H} - 1)}{8\beta^3}, \\
\Gamma^8 = & \frac{361}{2704\beta^2} - \frac{1}{208\beta^2}\Big(888\beta H^2 \\
& + 1776\alpha\beta H^2 R + 544\beta\dot{H} \\
& + 1232\alpha\beta H\dot{R} + 1088\alpha\beta\dot{H}\dot{R} \\
& - 136\alpha\beta\dot{R}^2 + 12\alpha\beta\dot{R}^2 - 544\alpha\beta\ddot{R} + 5\Big) \\
& + \frac{1}{624\beta^3}\Big(5\beta + 888\beta^2 H^2 + 1776\alpha\beta^2 H^2 R \\
& + 544\beta^2 \dot{H} + 1088\alpha\beta^2 \dot{H}\dot{R} + 1232\alpha\beta^2 H\dot{R} \\
& - 136\alpha\beta^2 \dot{R}^2 + 12\alpha\beta^2 \dot{R}^2 - 544\alpha\beta^2 \ddot{R}\Big), \\
\Gamma^9 = & \Big[4585\beta^2 + 4584960\beta^4 H^4 + 18339840\alpha^2\beta^4 H^4 \dot{R}^2 \\
& + 18339840\alpha\beta^4 H^4 \dot{R} + 26959872 \\
& \times \alpha^2\beta^4 H^3 \dot{R}\dot{R} + 13479936\alpha\beta^4 H^3 \ddot{R} \\
& + 4859904\beta^4 H^2 \dot{H} - 249312\beta^3 H^2 + 626688\alpha^2\beta^4 \\
& \times H^2 \dot{R}^3 + 19439616\alpha^2\beta^4 H^2 \dot{H}\dot{R}^2 \\
& - 1214976\alpha\beta^4 H^2 \dot{R}^2 - 2429952\alpha^2\beta^4 H^2 \dot{R}^3 \\
& + 313344 \times \alpha\beta^4 H^2 \dot{R}^2 + 9914368\alpha^2\beta^4 H^2 \ddot{R}^2 \\
& + 19439616\alpha\beta^4 H^2 \dot{H}\dot{R} - 4859904\alpha\beta^4 H^2 \ddot{R} \\
& - 9719808 \\
& \times \alpha^2\beta^4 H^2 \dot{R}\ddot{R} - 498624\alpha\beta^3 H^2 \dot{R} + 1294336\beta^4 \dot{H}^2 \\
& - 122240\beta^3 \dot{H} + 325632\alpha^2\beta^4 \dot{H}\dot{R}^3 \\
& + 5177344\alpha^2\beta^4 \dot{H}^2 \dot{R}^2 + 463872\alpha^2\beta^4 H\dot{R}^2 \dot{R} \\
& - 1294336\alpha^2\beta^4 \dot{H}\dot{R}^3 - 647168\alpha\beta^4 \dot{H}\dot{R}^2 \\
& + 162816\alpha\beta^4 \dot{H}\dot{R}^2 - 1782784\alpha^2\beta^4 H\dot{R}^2 \dot{R} \\
& + 14262272\alpha^2\beta^4 H\dot{H}\dot{R}\dot{R} + 5177344\alpha\beta^4 \dot{H}^2 \dot{R} \\
& + 7131136\alpha\beta^4 H\dot{H}\dot{R} - 5177344\alpha^2\beta^4 \dot{H}\dot{R}\ddot{R} \\
& - 2588672\alpha\beta^4 \dot{H}\ddot{R} - 7131136\alpha^2\beta^4 H\dot{R}\dot{\ddot{R}} \\
& - 244480\alpha\beta^3 \dot{H}\dot{R} - 376384\alpha\beta^3 H\dot{R} + 5760\alpha^2\beta^4 \dot{R}^4 \\
& + 80896\alpha\beta^4 \dot{R}^4 - 40704\alpha^2\beta^4 \dot{R}^4 \\
& + 647168\alpha^2\beta^4 \dot{R}^2 \ddot{R} - 162816\alpha^2\beta^4 \dot{R}^2 \dot{\ddot{R}}
\end{aligned}$$

$$\begin{aligned}
& +30560\alpha\beta^3\mathcal{R}^2 - 10992\alpha\beta^3\mathcal{R}^2 + 1294336\alpha \\
& \times\beta^4\ddot{\mathcal{R}}^2 + 122240\alpha\beta^3\ddot{\mathcal{R}}\Big], \\
\Gamma^{10} = & \Big[\Big(9980928(24336\mathcal{R}^2\alpha^2\beta H^4 + 24336\mathcal{R}\alpha\beta H^4 \\
& + 6084\beta H^4 + 36192\mathcal{R}\alpha^2\beta\dot{H}^3 \\
& + 18096\alpha\beta\dot{H}^3 + 13456\alpha^2\beta\dot{H}^2 H^2 \\
& - 240\mathcal{R}\alpha H^2 - 3120\mathcal{R}^3\alpha^2\beta H^2 - 1560\alpha\mathcal{R}^2\beta H^2 \\
& + 936\mathcal{R}^3\alpha^2\beta H^2 + 468\mathcal{R}^2\alpha\beta H^2 \\
& + 24960\mathcal{R}^2\alpha^2\beta\dot{H} H^2 + 24960\mathcal{R}\alpha\beta\dot{H} H^2 \\
& + 6240\beta\dot{H} H^2 - 12480\mathcal{R}\alpha^2\beta\ddot{H} H^2 - 6240\beta\alpha\ddot{H} H^2 \\
& - 120H^2 - 240\alpha\dot{H} H - 2320\alpha^2\mathcal{R}^2\beta\dot{H} H + 696\mathcal{R}^2 \\
& \times\alpha^2\beta\dot{H} H + 18560\mathcal{R}\alpha^2\beta\dot{H}\dot{H} H + 9280\alpha\beta\dot{H}\dot{H} H \\
& - 9280\alpha\beta\dot{H}\alpha\ddot{H} H + 6400\mathcal{R}^2\alpha^2\beta\dot{H}^2 \\
& + 6400\mathcal{R}\alpha\beta\dot{H}^2 + 1600\beta\dot{H}^2 + 1600\alpha\beta\ddot{H}^2 - 20\mathcal{R}^2\alpha \\
& - 60\alpha^2\mathcal{R}^4\beta + 9\mathcal{R}^4\alpha^2\beta + 100\mathcal{R}^4\alpha\beta \\
& - 1600\mathcal{R}^3\alpha^2\beta\dot{H} - 800\alpha\mathcal{R}^2\beta\dot{H} + 480\mathcal{R}^3\alpha^2\beta\dot{H} \\
& + 240\mathcal{R}^2\alpha\beta\dot{H} - 240\mathcal{R}^2\alpha^2\beta\ddot{H} - 6400\mathcal{R} \\
& \times\alpha\beta\dot{H}\alpha\ddot{H} - 3200\beta\dot{H}\alpha\ddot{H} + 800\mathcal{R}^2\alpha^2\beta\ddot{H}\Big)\beta^3 \\
& + 359424(804\mathcal{R}\alpha\beta H^2 + 402\beta H^2 + 524\alpha \\
& \times\beta\dot{H} H - 70\alpha\mathcal{R}^2\beta - 3\mathcal{R}^2\alpha\beta + 560\mathcal{R}\alpha\beta\dot{H} \\
& + 280\beta\dot{H} - 280\beta\alpha\ddot{H} - 10\Big)^2\beta^3 - 239616 \\
& \times(888H^2\beta^2 - 136\alpha\mathcal{R}^2\beta^2 + 12\mathcal{R}^2\alpha\beta^2 \\
& + 1776\mathcal{R}^2\alpha\beta^2 + 1088\mathcal{R}\alpha\dot{H}\beta^2 \\
& + 544\dot{H}\beta^2 \\
& + 1232H\alpha\dot{H}\beta^2 - 544\alpha\ddot{H}\beta^2 + 5\beta\Big)\beta^2 + 128 \\
& (888H^2\beta^2 - 136\alpha\mathcal{R}^2\beta^2 + 12\mathcal{R}^2\alpha\beta^2 + 1776H^2 \\
& \times\mathcal{R}\alpha\beta^2 + 1088\mathcal{R}\alpha\dot{H}\beta^2 + 544\dot{H}\beta^2 + 1232H\alpha\dot{H}\beta^2 \\
& - 544\alpha\ddot{H}\beta^2 + 5\beta\Big)^3 + \Big(4(73359360 \\
& \times H^4\beta^4 - 38879232H^2\mathcal{R}^3\alpha^2\beta^4 + 92160\mathcal{R}^4\alpha^2\beta^4 \\
& + 10027008H^2\mathcal{R}^3\alpha^2\beta^4 + 293437440H^4 \\
& \times\mathcal{R}^2\alpha^2\beta^4 + 82837504\mathcal{R}^2\alpha^2\dot{H}^2\beta^4 \\
& + 82837504\mathcal{R}\alpha\dot{H}^2\beta^4 + 20709376\dot{H}^2\beta^4 \\
& + 158629888 \times H^2\alpha^2\dot{H}^2\beta^4 + 20709376\alpha\ddot{H}^2\beta^4 \\
& + 1294336\mathcal{R}^4\alpha\beta^4 + 19439616H^2\mathcal{R}^2\alpha\beta^4 + 5013504 \\
& \times H^2\mathcal{R}^2\alpha\beta^4 + 293437440H^4\mathcal{R}\alpha\beta^4 \\
& + 651264\mathcal{R}^4\alpha^2\beta^4 + 77758464H^2\dot{H}\beta^4 - 10354688 \\
& \times\alpha\mathcal{R}^2\dot{H}\beta^4 + 5210112\mathcal{R}^3\alpha^2\dot{H}\beta^4 \\
& + 311033856H^2\mathcal{R}^2\alpha^2\dot{H}\beta^4 + 2605056\mathcal{R}^2\alpha\dot{H}\beta^4 \\
& + 311033856H^2\mathcal{R}\alpha\dot{H}\beta^4 + 20709376\mathcal{R}^3\alpha^2\dot{H}\beta^4 \\
& + 7421952H\mathcal{R}^2\alpha^2\dot{H}\beta^4 + 431357952 \\
& \times H^3\mathcal{R}\alpha^2\dot{H}\beta^4 - 28524544H\alpha\alpha\mathcal{R}^2\dot{H}\beta^4 \\
& + 215678976H^3\alpha\dot{H}\beta^4 \\
& + 228196352H\mathcal{R}\alpha^2\dot{H}\dot{H} \\
& \times\beta^4 + 114098176H\alpha\dot{H}\beta^4 - 77758464H^2\alpha\ddot{H}\beta^4 \\
& + 10354688\mathcal{R}^2\alpha^2\dot{H}\beta^4 - 2605056\mathcal{R}^2 \\
& \times\alpha^2\dot{H}\beta^4 - 155516928H^2\mathcal{R}\alpha^2\ddot{H}\beta^4 - 82837504\mathcal{R}\alpha\dot{H} \\
& \alpha\ddot{H}\beta^4 - 41418752\dot{H}\alpha\ddot{H}\beta^4 \\
& - 114098176H\alpha^2\dot{H}\dot{H}\beta^4 + 3988992H^2\beta^3 \\
& + 488960\mathcal{R}^2\alpha\beta^3 + 175872\mathcal{R}^2\alpha\beta^3 + 7977984H^2 \\
& \times\mathcal{R}\alpha\beta^3 - 3911680\mathcal{R}\alpha\dot{H}\beta^3 + 1955840\dot{H}\beta^3 \\
& - 6022144H\alpha\dot{H}\beta^3 + 1955840\alpha\ddot{H}\beta^3 \\
& + 73360\beta^2\Big)^3 + \Big(9980928(24336\mathcal{R}^2\alpha^2\beta H^4 \\
& + 24336\mathcal{R}\alpha\beta H^4 + 6084\beta H^4 + 36192\mathcal{R}\alpha^2\beta
\end{aligned}$$

$$\begin{aligned}
& \times \dot{\mathcal{R}} H^3 + 18096\alpha\beta\dot{\mathcal{R}} H^3 + 13456\alpha^2\beta\dot{\mathcal{R}}^2 H^2 \\
& - 240\mathcal{R}\alpha H^2 - 3120\mathcal{R}^3\alpha^2\beta H^2 - 1560\alpha\mathcal{R}^2 \\
& \times \beta H^2 + 936\mathcal{R}^3\alpha^2\beta H^2 + 468\mathcal{R}^2\alpha\beta H^2 \\
& + 24960\mathcal{R}^2\alpha^2\beta\dot{H} H^2 + 24960\mathcal{R}\alpha\beta\dot{H} H^2 \\
& + 6240 \times \beta\dot{H} H^2 - 12480\mathcal{R}\alpha^2\beta\ddot{\mathcal{R}} H^2 \\
& - 6240\beta\alpha\ddot{\mathcal{R}} H^2 - 120H^2 - 240\alpha\dot{\mathcal{R}} H \\
& - 2320\alpha^2\mathcal{R}^2\beta\dot{\mathcal{R}} H + 696\mathcal{R}^2\alpha^2\beta\dot{\mathcal{R}} H \\
& + 18560\mathcal{R}\alpha^2\beta\dot{H}\dot{\mathcal{R}} H \\
& + 9280\alpha\beta\dot{H}\dot{\mathcal{R}} H - 9280\alpha\beta\dot{R} \\
& \alpha\ddot{\mathcal{R}} H + 6400\mathcal{R}^2\alpha^2\beta\dot{H}^2 + 6400\mathcal{R}\alpha\beta\dot{H}^2 + 1600\beta\dot{H}^2 \\
& + 1600\alpha\beta\ddot{\mathcal{R}}^2 - 20\mathcal{R}^2\alpha - 60\mathcal{R}^4\alpha^2\beta \\
& + 9\mathcal{R}^4\alpha^2\beta + 100\mathcal{R}^4\alpha\beta \\
& - 1600\mathcal{R}^3\alpha^2\beta\dot{H} - 800\alpha\mathcal{R}^2\beta\dot{H} + 480\mathcal{R}^3\alpha^2\beta\dot{H} \\
& + 240\mathcal{R}^2\alpha\beta\dot{H} - 240\mathcal{R}^2\alpha^2\beta\ddot{\mathcal{R}} - 6400\mathcal{R}\alpha^2 \\
& \times \beta\dot{H}\ddot{\mathcal{R}} - 3200\beta\dot{H}\alpha\ddot{\mathcal{R}} + 800\mathcal{R}^2\alpha^2\beta\ddot{\mathcal{R}}) \\
& \beta^4 + 359424(804\mathcal{R}\alpha\beta H^2 + 402\beta H^2 + 524\alpha\beta\dot{\mathcal{R}} H \\
& - 70\alpha\mathcal{R}^2\beta - 3\mathcal{R}^2\alpha\beta + 560\mathcal{R}\alpha\beta\dot{H} \\
& + 280\beta\dot{H} - 280\beta\alpha\ddot{\mathcal{R}} - 10)^2\beta^3 - 239616(888H^2\beta^2 \\
& - 136\alpha\mathcal{R}^2\beta^2 + 12\mathcal{R}^2\alpha\beta^2 + 1776H^2\mathcal{R}\alpha\beta^2 \\
& + 1088\mathcal{R}\alpha\dot{H}\beta^2 + 544\dot{H}\beta^2 + 1232H\alpha\dot{\mathcal{R}}\beta^2 \\
& - 544\alpha\ddot{\mathcal{R}}\beta^2 + 5\beta)(24336\mathcal{R}^2\alpha^2\beta H^4 + 24336\mathcal{R}\alpha\beta H^4 \\
& + 6084\beta H^4 + 36192\mathcal{R}\alpha^2\beta\dot{\mathcal{R}} H^3 \\
& + 18096\alpha\beta\dot{\mathcal{R}} H^3 + 13456\alpha^2\beta\dot{\mathcal{R}}^2 H^2 - 240\mathcal{R}\alpha H^2 \\
& - 3120\mathcal{R}^3\alpha^2\beta H^2 \\
& - 1560\alpha\mathcal{R}^2\beta H^2 + 936\mathcal{R}^3\alpha^2\beta H^2 \\
& + 468\mathcal{R}^2\alpha\beta H^2 + 24960\mathcal{R}^2\alpha^2\beta\dot{H} H^2 \\
& + 24960\mathcal{R}\alpha\beta\dot{H} H^2 + 6240\beta\dot{H} H^2 \\
& - 12480\mathcal{R}\alpha^2\beta\ddot{\mathcal{R}} H^2 - 6240\beta\alpha\ddot{\mathcal{R}} H^2 \\
& - 120H^2 - 240\alpha\dot{\mathcal{R}} H - 2320\alpha^2\mathcal{R}^2\beta\dot{\mathcal{R}} H + 696\mathcal{R}^2\alpha^2 \\
& \times \beta\dot{\mathcal{R}} H + 18560\mathcal{R}\alpha^2\beta\dot{H}\dot{\mathcal{R}} H + 9280\alpha\beta\dot{H}\dot{\mathcal{R}} H \\
& - 9280\alpha\beta\dot{\mathcal{R}}\alpha\ddot{\mathcal{R}} H + 6400\mathcal{R}^2\alpha^2\beta\dot{H}^2 \\
& + 6400\mathcal{R}\alpha\beta\dot{H}^2 + 1600\beta\dot{H}^2 + 1600\beta\alpha\ddot{\mathcal{R}}^2 \\
& - 20\mathcal{R}^2\alpha - 60\mathcal{R}^4\alpha^2\beta + 9\mathcal{R}^4\alpha^2\beta + 100\mathcal{R}^4\alpha\beta \\
& - 1600\mathcal{R}^3\alpha^2\beta\dot{H} - 800\alpha\mathcal{R}^2\beta\dot{H} + 480\mathcal{R}^3\alpha^2\beta\dot{H} \\
& + 240\mathcal{R}^2\alpha\beta\dot{H} - 240\mathcal{R}^2\alpha^2\beta\ddot{\mathcal{R}} \\
& - 6400\mathcal{R} \times \alpha^2\beta\dot{H}\ddot{\mathcal{R}} - 3200\beta\dot{H}\alpha\ddot{\mathcal{R}} \\
& + 800\mathcal{R}^2\alpha^2\beta\ddot{\mathcal{R}})\beta^3 - 87552(804\mathcal{R}\alpha\beta H^2 + 402\beta H^2 \\
& + 524\alpha\beta \times \dot{\mathcal{R}} H - 70\alpha\mathcal{R}^2\beta - 3\mathcal{R}^2\alpha\beta + 560\mathcal{R}\alpha\beta\dot{H} \\
& + 280\beta\dot{H} \\
& - 280\beta\alpha\ddot{\mathcal{R}} - 10)(888H^2\beta^2 \\
& - 136\alpha\mathcal{R}^2\beta^2 + 12\mathcal{R}^2\alpha\beta^2 + 1776H^2\mathcal{R}\alpha\beta^2 \\
& + 1088\mathcal{R}\alpha\dot{H}\beta^2 + 544\dot{H}\beta^2 + 1232H\alpha\dot{\mathcal{R}}\beta^2 \\
& - 544\alpha\ddot{\mathcal{R}}\beta^2 + 5\beta)\beta^2 + 128(888H^2\beta^2 \\
& - 136\alpha\mathcal{R}^2\beta^2 + 12\mathcal{R}^2\alpha\beta^2 + 1776H^2\mathcal{R}\alpha\beta^2 \\
& + 1088\mathcal{R}\alpha\dot{H}\beta^2 + 544\dot{H}\beta^2 \\
& + 1232H\alpha\dot{\mathcal{R}}\beta^2 - 544\alpha\ddot{\mathcal{R}}\beta^2 \\
& + 5\beta)^3) \Big)^{\frac{1}{2}} \Big)^{\frac{1}{3}} \Big], \\
\Gamma^{11} &= \frac{361}{1352\beta^2} - \frac{1}{208\beta^2} \Big[-136\alpha\mathcal{R}^2\beta - 544\alpha\ddot{\mathcal{R}}\beta \\
& + 888\beta H^2 + 1776\alpha\beta H^2\mathcal{R} + 544\beta\dot{H} \\
& + 1232\alpha\beta H\dot{\mathcal{R}} + 1088\alpha\beta\dot{H}\mathcal{R} + 12\alpha\beta\mathcal{R}^2 + 5 \Big] \\
& - \frac{1}{624\beta^3} \Big[-136\alpha\mathcal{R}^2\beta^2 - 544\alpha\ddot{\mathcal{R}}\beta^2 + 5\beta \\
& + 888\beta^2 H^2 + 1776\alpha\beta^2 H^2\mathcal{R} + 544\beta^2\dot{H} \\
& + 1088\alpha\beta^2\dot{H}\mathcal{R} + 1232\alpha\beta^2 H\dot{\mathcal{R}} + 12\alpha\beta^2\mathcal{R}^2 \Big], \\
\Gamma^{12} &= \frac{6859}{17576\beta^3} - \frac{1}{26\beta^3} \Big[70\alpha\mathcal{R}^2\beta - 402\beta H^2 \\
& - 804\alpha\beta H^2\mathcal{R} - 280\beta\dot{H} - 524\alpha\beta H\dot{\mathcal{R}} \\
& - 560\alpha\beta\dot{H}\mathcal{R} + 3\alpha\beta\mathcal{R}^2 + 280\alpha\beta\ddot{\mathcal{R}} + 10 \Big] \\
& - \frac{19}{1352\beta^3} \Big[888\beta H^2 + 1776\alpha\beta H^2\mathcal{R} \\
& + 544\beta\dot{H} + 1232\alpha\beta H\dot{\mathcal{R}} + 1088\alpha\beta\dot{H}\mathcal{R} - 136\alpha\beta\mathcal{R}^2 \\
& + 12\alpha\beta\mathcal{R}^2 - 544\alpha\beta\ddot{\mathcal{R}} + 5 \Big], \\
\Gamma^{13} &= \frac{361}{2704\beta^2} - \frac{1}{208\beta^2} \Big[-136\alpha\mathcal{R}^2\beta - 544\alpha\ddot{\mathcal{R}}\beta \\
& + 888\beta H^2 + 1776\alpha\beta H^2\mathcal{R} + 544\beta\dot{H} \\
& + 1232\alpha\beta H\dot{\mathcal{R}} + 1088\alpha\beta\dot{H}\mathcal{R} + 12\alpha\beta\mathcal{R}^2 + 5 \Big] \\
& + \frac{1}{624\beta^3} \Big[-136\alpha\mathcal{R}^2\beta^2 - 544\alpha\ddot{\mathcal{R}}\beta^2 \\
& + 5\beta + 888\beta^2 H^2 + 1776\alpha\beta^2 H^2\mathcal{R} + 544\beta^2\dot{H} \\
& + 1088\alpha\beta^2\dot{H}\mathcal{R} + 1232\alpha\beta^2 H\dot{\mathcal{R}} + 12\alpha\beta^2\mathcal{R}^2 \Big], \\
\Gamma^{14} &= \frac{6859}{17576\beta^3} - \frac{1}{26\beta^3} \Big[70\alpha\mathcal{R}^2\beta \\
& + 280\alpha\ddot{\mathcal{R}}\beta - 402\beta H^2 - 804\alpha\beta H^2\mathcal{R} - 280\beta\dot{H} \\
& - 524\alpha\beta H\dot{\mathcal{R}} - 560\alpha\beta\dot{H}\mathcal{R} + 3\alpha\beta\mathcal{R}^2 + 10 \Big] \\
& - \frac{19}{1352\beta^3} \Big[-136\alpha\mathcal{R}^2\beta - 544\alpha\ddot{\mathcal{R}}\beta
\end{aligned}$$

$$+888\beta H^2 + 1776\alpha\beta H^2\mathcal{R} + 544\beta\dot{H} \\ +1232\alpha\beta H\dot{\mathcal{R}} + 1088\alpha\beta\dot{H}\mathcal{R} + 12\alpha\beta\mathcal{R}^2 + 5 \Big].$$

References

1. H.A. Buchdahl, Mon. Not. Roy. Astron. Soc. **150**, 1 (1970)
2. S. Capozziello, V.F. Cardone, A. Troisi, Phys. Rev. D **71**, 043503 (2005)
3. G. Cognola et al., Phys. Rev. D **77**, 046009 (2008)
4. A.D. Felice, S.R. Tsujikawa, Living Rev. Relativ. **13**, 161 (2010)
5. E.V. Linder, Phys. Rev. D **81**, 127301 (2010)
6. Y.F. Cai et al., Prog. Phys. **79**, 106901 (2016)
7. S. Nojiri, S.D. Odintsov, V.K. Oikonomou, Phys. Rep. **692**, 104 (2017)
8. M. Sharif, M.Z. Gul, Eur. Phys. J. Plus **133**, 345 (2018)
9. M. Sharif, M.Z. Gul, Int. J. Mod. Phys. D **28**, 1950054 (2019)
10. M. Sharif, M.Z. Gul, Chin. J. Phys. **57**, 329 (2019)
11. M.Z. Gul, M. Sharif, New Astron. **106**, 102137 (2024)
12. M. Sharif, M.Z. Gul, Ann. Phys. **465**, 169674 (2024)
13. M. Sharif, M.Z. Gul, Phys. Scr. **99**, 065036 (2024)
14. M. Sharif, M.Z. Gul, I. Hashim, Phys. Dark Univ. **46**, 101606 (2024)
15. M.Z. Gul, M. Sharif, I. Hashim, Phys. Dark Univ. **45**, 101537 (2024)
16. M.Z. Gul, M. Sharif, Phys. Scr. **99**, 055036 (2024)
17. M.Z. Gul, M. Sharif, Chin. J. Phys. **88**, 388 (2024)
18. M.Z. Gul, M. Sharif, I. Kanwal, New Astron. **109**, 102204 (2024)
19. N. Katirci, M. Kavuk, Eur. Phys. J. Plus **129**, 163 (2014)
20. D.M. Pandya, V.O. Thomas, R. Sharma, Astrophys. Space Sci. **356**, 292 (2015)
21. M. Roshan, F. Shojaei, Phys. Rev. D **94**, 044002 (2016)
22. C.V.R. Board, J.D. Barrow, Phys. Rev. D **96**, 123517 (2017)
23. O. Akarsu, N. Katirci, S. Kumar, Phys. Rev. D **97**, 024011 (2018)
24. N. Nari, M. Roshan, Phys. Rev. D **98**, 024031 (2018)
25. P.H.R.S. Moraes, P.K. Sahoo, Phys. Rev. D **97**, 024007 (2018)
26. S. Bahamonde, M. Marciu, P. Rudra, Phys. Rev. D **100**, 083511 (2019)
27. S. Bahamonde, M. Marciu, P. Rudra, Phys. Rev. D **100**, 083511 (2019)
28. C. Ranjit, P. Rudra, S. Kundu, Ann. Phys. **428**, 168432 (2021)
29. G. Mustafa et al., Phys. Scr. **96**, 105008 (2021). ibid. 045009
30. G. Mustafa et al., Chin. J. Phys. **77**, 1742 (2022)
31. F. Javed, Int. J. Geom. Methods Mod. Phys. **19**, 2250190 (2022)
32. F. Javed et al., Nucl. Phys. B **990**, 116180 (2023)
33. F. Javed et al., Fortschr. Phys. **2023**, 2200214 (2023)
34. F. Javed et al., Eur. Phys. J. C **83**, 1088 (2023)
35. F. Javed, Eur. Phys. J. C **83**, 513 (2023)
36. F. Javed, Ann. Phys. **458**, 169464 (2023)
37. M. Adeel et al., Mod. Phys. Lett. A **38**, 2350152 (2023)
38. A. Waseem et al., Eur. Phys. J. C **83**, 1088 (2023)
39. M.Z. Gul, M. Sharif, A. Arooj, Fortschr. Phys. **72**, 2300221 (2024)
40. M.Z. Gul, M. Sharif, A. Arooj, Phys. Scr. **99**, 045006 (2024)
41. M.Z. Gul, M. Sharif, A. Arooj, Gen. Relativ. Gravit. **56**, 45 (2024)
42. M.Z. Gul et al., Eur. Phys. J. C **84**, 775 (2024)
43. M.Z. Gul et al., Eur. Phys. J. C **84**, 8 (2024)
44. S. Rani et al., Int. J. Geom. Methods Mod. Phys. **21**, 2450033 (2024)
45. M. Sharif, M.Z. Gul, Phys. Scr. **96**, 025002 (2021)
46. M. Sharif, M.Z. Gul, Eur. Phys. J. Plus **136**, 503 (2021)
47. M. Sharif, M.Z. Gul, Mod. Phys. Lett. A **36**, 2150214 (2021)
48. M. Sharif, M.Z. Gul, Phys. Scr. **96**, 125007 (2021)
49. M. Sharif, M.Z. Gul, Adv. Astron. **2021**, 6663502 (2021)
50. M. Sharif, M.Z. Gul, Chin. J. Phys. **71**, 35 (2021)
51. M. Sharif, M.Z. Gul, Universe **96**, 154 (2021)
52. M. Sharif, M.Z. Gul, Int. J. Mod. Phys. A **36**, 2150004 (2021)
53. M. Sharif, M.Z. Gul, Mod. Phys. Lett. A **19**, 2250005 (2022)
54. M. Sharif, M.Z. Gul, Fortschr. Phys. **71**, 2200184 (2023)
55. M. Sharif, M.Z. Gul, Gen. Relativ. Gravit. **55**, 10 (2023)
56. M. Sharif, M.Z. Gul, Phys. Scr. **98**, 035030 (2023)
57. M.Z. Gul, M. Sharif, A. Afzal, Chin. J. Phys. **89**, 1347 (2024)
58. J.M. Senovilla, Gen. Relativ. Gravit. **30**, 701 (1998)
59. A.R. Liddle, J. High Energy Phys. **260**, 3 (1998)
60. M. Bojowald, Phys. Rev. Lett. **86**, 5227 (2001)
61. M. Bojowald, Gen. Relativ. Gravit. **40**, 2659 (2008)
62. V. Bozza, M. Bruni, J. Cosmol. Astropart. Phys. **2009**, 014 (2009)
63. Y.F. Cai, D.A. Easson, R. Brandenberger, J. Cosmol. Astropart. Phys. **2012**, 020 (2012)
64. Y.F. Cai, Sci. China Phys. Mech. Astron. **57**, 1414 (2014)
65. K. Bamba, A.N. Makarenko, A.N. Myagky, S.I. Nojiri, S.D. Odintsov, J. Cosmol. Astropart. Phys. **2014**, 008 (2014)
66. K. Bamba, A.N. Makarenko, A.N. Myagky, S.D. Odintsov, Phys. Lett. B **732**, 349 (2014)
67. A.R. Amani, Int. J. Mod. Phys. D **25**, 1650071 (2016)
68. J. De Haro, J. Amorós, Phys. Rev. D **97**, 064014 (2018)
69. S.K. Tripathy, B. Mishra, S. Ray, R. Sengupta, Chin. J. Phys. **71**, 610 (2021)
70. H. Shabani, A.H. Ziae, Eur. Phys. J. C **78**, 1 (2018)
71. M. Caruana, G. Farrugia, J. Levi Said, Eur. Phys. J. C **80**, 640 (2020)
72. N. Ahmed, T.M. Kamel, M.I. Nouh, Rev. Mex. Astron. Astrofis. **58**, 245 (2022)
73. M. Zubair, Q. Muneer, S. Waheed, Int. J. Mod. Phys. D **31**, 2250092 (2022)
74. M.G. Ganiou et al., Eur. Phys. J. Plus **137**, 208 (2022)
75. J.K. Singh, A. Singh, A. Beesham, H. Shabani, Ann. Phys. **455**, 169382 (2023)
76. M. Sharif, M.Z. Gul, N. Fatima, Chin. J. Phys. **91**, 66 (2024)
77. M. Sharif, M.Z. Gul, N. Fatima, New Astron. **109**, 102211 (2024)
78. M.Z. Gul, M. Sharif, S. Shabbir, Eur. Phys. J. C **84**, 802 (2024)
79. V. Faraoni, Phys. Rev. D **80**, 124040 (2009)
80. A.A. Starobinsky, Phys. Lett. B **91**, 99 (1980)
81. G. Navó, E. Elizalde, Int. J. Geom. Methods Mod. Phys. **17**, 2050162 (2020)
82. A. De la Cruz-Dombriz, D. Sáez-Gómez, Class. Quantum Gravity **29**, 245014 (2012)